Nanoparticles

DOI: 10.1002/anie.200701344

Unusual Nanoparticle Structures from the Silica Sol–Gel-Mediated Self-Assembly of a Prussian-Blue Analogue and the Formation of Templated Graphite Regions**

*Joshua G. Moore, Eric J. Lochner, and Albert E. Stiegman**

The formation of nanodimensional inorganic structures of differing size and aspect ratio is of interest for optical, magnetic, and electronic applications. Their preparation is accomplished by several methods including arrested precipitation, synthesis in a nanoporous matrix, and the use of molecular precursors. We have found that the self-assembly of an analogue of the Prussian-blue class of coordination polymers could be effectively mediated by the competitive gelation of a silica sol–gel medium to yield entrapped superparamagnetic nanoparticles.[1] One implication of this result was that it suggested a direct one-pot synthetic method for the production of entrapped nanoparticles for some of the aforementioned applications. To realize this approach, however, the process must be able to controllably produce nanoparticles of a diverse morphology. We report herein the observation and characterization of nanocrystalline rods and disks formed from the competition between the self-assembly of the Prussian-Blue analogue $K^{I}_{X}Ni^{II}_{Y}[Fe^{III}(CN)_6]$ and gelation of a silica sol–gel medium. The origin of these different particle morphologies as a function of the process is not completely known but details of their structure suggest a synergistic interaction between the assembling coordination polymer and the polymerizing silica.

Incorporating Ni^{II} ions with potassium ferricyanide during the solution phase of the silica sol–gel process yielded homogeneous silica xerogel monoliths containing the Ni^{II}/Fe^{III} Prussian-blue complex. Conditions under which a maximum amount of the Prussian-blue complex could be incorporated without incurring precipitation were determined from systematic variations in the water/co-solvent ratio and the concentration of the cation and anion. At concentrations up to 0.1 mol% total metal to silicon (Fe + Ni/Si), the solution remained transparent through gelation, aging, and drying, ultimately yielding a homogeneous optically transparent xerogel (Supporting Information, Figure S1).

Imaging of a 0.1 mol% $K^{I}_{X}Ni^{II}_{Y}[Fe^{III}(CN)_6]$ xerogel composite using transition electron microscopy (TEM) reveals unusual nanorod structures sequestered in the glass. Figure 1a shows a representative example, the dimension of

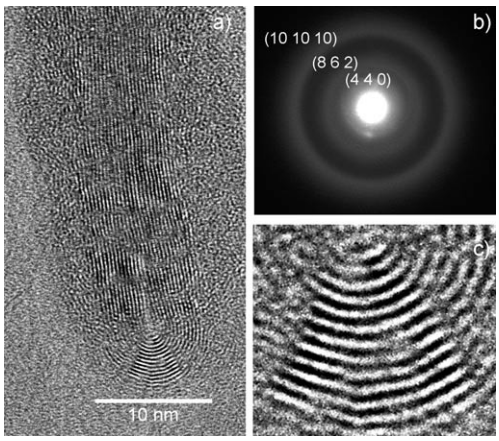

Figure 1. a) TEM image of $K^{I}_{X}Ni^{II}_{Y}[Fe^{III}(CN)_6]$ nanorod in silica xerogel, b) indexed electron diffraction pattern from a region containing isotropically distributed nanorods, and c) expanded view of the end-capped region of the nanorod.

which is 13 × 35 nm. While a complete statistical analysis was not undertaken owing to the excessive TEM time required, most of the rods observed at this concentration were of similar size with average dimensions of approximately 15 × 40 nm. Energy dispersive X-ray spectroscopy (EDS) of the nanorod regions of the TEM image verified the presence of Ni, Fe, and K. Bulk $K^{I}_{X}Ni^{II}_{Y}[Fe^{III}(CN)_6]$ crystallizes in a face centered cubic lattice with the space group *Fm*3*m*.[2–4] The TEM image itself shows well-resolved lattice planes, the measured spacing between them is 0.33(±0.02) nm, which is assigned to the (220) plane of the $K^{I}_{X}Ni^{II}_{Y}[Fe^{III}(CN)_6]$ crystal. Also consistent with crystalline order is an electron diffraction ring pattern observed from a region of the material containing multiple nanorods. The high-angle reflections from the TEM electron diffraction rings could be indexed

[*] Dr. J. G. Moore, Dr. A. E. Stiegman
Department of Chemistry and Biochemistry
Florida State University
Tallahassee, FL 32303 (USA)
Fax: (+1) 850-644-8281
E-mail: stiegman@chem.fsu.edu
Dr. E. J. Lochner
The Materials Research and Technology Center (MARTECH)
Florida State University
Tallahassee, FL 32303 (USA)

[**] Funding was provided by the Air Force Office of Scientific Research through MURI 1606U8 and by AFRL/MN under grant No. FA8651-05-1-0002. J.G.M. was supported by a grant from MARTECH. We thank Dr. Yan Xin at the TEM facility of the National High Magnetic Field Laboratory where work was supported under NSF grant No. DMR-9625692. We also thank Kim Riddle of the Biological Science Imaging Resource.

Supporting information for this article is available on the WWW under http://www.angewandte.org or from the author.

(Figure 1b) to the more intense high-angle diffractions of the bulk material. The unit-cell length calculated from the diffraction rings is 1.02 nm, which is consistent with the lattice parameter of the bulk phase of 1.0232 nm that was reported for materials made with the 1:1 Ni:Fe ratio used in our materials.[5]

All of the observed nanorods are capped which may arise through folding of the rods as a result of forces imposed on the structure by gelation (i.e. cross-linking of the silica around the particle), however, all of the rods are capped at both ends which would be inconsistent with a rod folding over on itself. Moreover, the interplanar spacing measured across the diameter of the rod through the center are relatively constant (i.e. there appears to be no void space at the center) which suggests that capping occurs at both ends and is part of the self-assembly process and may result from reconstruction of the surface as the concentration of free metal ions decreases and the viscosity of the medium increases limiting mass transport. In short, when the nanorod can no longer grow lengthwise the ends close off to minimize vacant coordination sites. Close inspection of the capped region (Figure 1c) shows facets consistent with reconstruction along defined crystallographic planes. At a lower concentration (0.05 mol%), fewer nanorods are observed and those present tend to be shorter. The species that predominate at this concentration are short rods or disk-like structures (Figure 2). Scrutiny of these structures indicates that spacing is observed consistent with the crystallographic planes of the Prussian-blue complex. Clearly, the predominance of these structures at a lower concentration suggests that the specific nanostructures that form at the solubility limit of the Prussian-blue analogue are dictated in large part by the amount of metal ions present. It also suggests that some level of synthetic control over the structures that form is possible. Notably, the observed rod-like structures differ significantly from Co^{II}- and Ni^{II}- Fe^{III} Prussian-blue nanoparticles produced by other means (e.g. microemusion).[5–7] This difference may arise from solution-phase interactions between the Ni^{II} ions with the sol–gel solution which may direct structure formation. In particular, prior studies have shown that complex formation occurs between Ni^{II} ions and silicate esters in the sol–gel medium.[8] Silicate coordination would occupy vacant coordination sites on the Ni^{II} and sterically restrict the direction of cyanide-bridge formation, much as blocking ligands are used to direct structure formation in supramolecular synthesis.[9,10]

Calcination of the nanoparticle–silica composites at 500 °C in air destroys the coordination complex and yields a brown, translucent glass. TEM imaging of the calcined material shows that the silica retains the imprint of the nanorods even after high-temperature processing (Figure 3a,

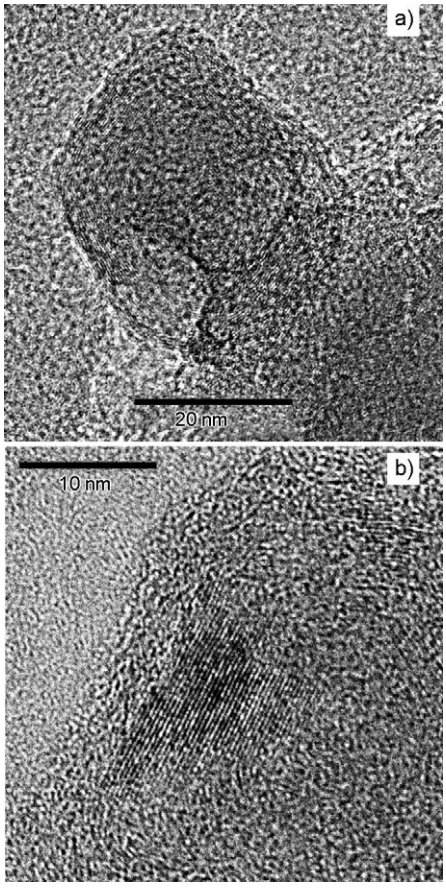

Figure 2. TEM images of $K^{I}_{x}Ni^{II}_{y}[Fe^{III}(CN)_6]$ Prussian-blue nanoparticles forming into a) disk and b) small rod structures at low concentration (0.05 mol%).

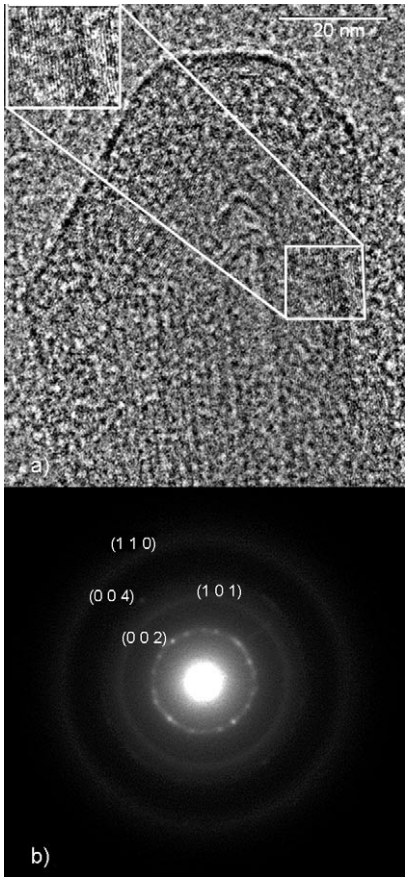

Figure 3. a) TEM image of the void region imprinted in the silica matrix by a $K^{I}_{x}Ni^{II}_{y}[Fe^{III}(CN)_6]$ nanoparticle after calcination at 500 °C, inset: enlarged view, and b) electron diffraction pattern of the void region.

for enlarged view and alternate voids regions see Supporting Information, Figures S2 and S3). Interestingly, crystallographic planes are resolved in the image of the imprinted region (Figure 3a, inset) which suggests that a crystalline phase has formed from the decomposition process on the surface of the void space. Relatively well-defined electron diffraction rings from these features further support the crystalline nature of this remaining phase (Figure 3b). The crystallographic planes are oriented coincident with the crystallographic planes of the original Prussian-blue complex. The interplanar spacing measured and averaged from 8–10 measurements of the better-resolved portions of different images was found to be 0.37 ± 0.06 nm. Calcinations of bulk Ni^{II}/Fe^{III} Prussian-blue have been reported where it was found that high-temperature processing under air results in a reductive decomposition of the complex into a crystalline fcc metallic Fe–Ni phase ($FeNi_3$) and amorphous carbonaceous material. A determination of the d-spacing from the electron diffraction rings indicates that the remaining crystalline phase is not $FeNi_3$, but is completely assignable to diffraction from crystalline graphite with the measured spacing in the TEM image therefore corresponding to the d_{002} interplanar spacing. In studies of the reductive decomposition of polyacrylonitrile in the nanoscale confines of porous Vycor glass, graphite nanocrystals were found to order with the graphitic planes (002) along the long direction of the pores.[11] The observation of oriented graphite formation from the decomposition of the Ni^{II}–Fe^{III} Prussian-blue nanorods may suggest a general tendency for thermally produced graphite to orient on the long direction of a silica pore, however, the fact that it appears to always follow the original direction of the (220) Prussian-blue crystal planes, even following facets that occur at oblique angles to the long direction of the nanorod suggests that the initial structure of the Prussian-blue nanorod may in some fashion dictate the final orientation of the resulting graphite.

In summary, the competing kinetics of silica condensation and the self-assembly of a Prussian-blue complex at the limits of its solubility produce an entrapped array of crystalline nanoscale complexes whose dimensions appear to be controlled by the amount of materials available to assemble the Prussian-blue complex and, possibly, by molecular interactions between the components. Calcination of the composite results in the destruction of the nanorods, and the production of a crystalline graphite in the void space along the surface of the silica. Taken together, the results suggest that control of competing kinetic processes can generate complex nanostructures in a one-pot synthesis and that subsequent processing can be successfully used to produce void structures containing other nanocrystallites.

Experimental Section

In the optimized preparation, an aqueous methanol (1/1 v/v) solution of potassium ferricyanide was added drop-wise to a solution of the nitrate salt of Ni^{II} and tetramethylorthosilicate in methanol (30.3 mL) to achieve a 1:1 Ni:Fe molar ratio at the desired concentration of the Prussian-blue complex. Aliquots of the solution (4 mL) were dispensed into disposable cuvettes (polystyrene), sealed, and allowed to gel. Gelation occurred after several days at which time the cuvettes were punctured with a needle and allowed to age and dry over a period of approximately 3 months.

Received: March 27, 2007
Revised: August 15, 2007
Published online: October 5, 2007

Keywords: graphite · nanoparticles · Prussian blue · self-assembly · sol–gel processes

[1] J. G. Moore, E. J. Lochner, C. Ramsey, N. S. Dalal, A. E. Stiegman, *Angew. Chem.* **2003**, *115*, 2847 – 2849; *Angew. Chem. Int. Ed.* **2003**, *42*, 2741 – 2743.
[2] S. Juszczyk, C. Johansson, M. Hanson, A. Ratuszna, G. Malecki, *J. Magn. Magn. Mater.* **1994**, *138*, 281 – 286.
[3] S. Juszczyk, C. Johansson, M. Hanson, A. Ratuszna, G. Malecki, *J. Phys. Condens. Matter* **1994**, *6*, 5697 – 5706.
[4] G. Malecki, A. Ratuszna, *Powder Diffr.* **1999**, *14*, 25 – 30.
[5] S. Yamada, K. Kuwabara, K. Koumoto, *Mater. Sci. Eng. B* **1997**, *49*, 89 – 94.
[6] P. Y. Chow, J. Ding, X. Z. Wang, C. H. Chew, L. M. Gan, *Phys. Status Solidi A* **2000**, *180*, 547 – 553.
[7] S. Vaucher, J. Fielden, M. Li, E. Dujardin, S. Mann, *Nano Lett.* **2002**, *2*, 225 – 229.
[8] R. E. Bossio, S. D. Callahan, A. E. Stiegman, A. G. Marshall, *Chem. Mater.* **2001**, *13*, 2097 – 2102.
[9] C. P. Berlinguette, J. R. Galan-Mascaros, K. R. Dunbar, *Inorg. Chem.* **2003**, *42*, 3416 – 3422.
[10] B. Moulton, M. J. Zaworotko, *Chem. Rev.* **2001**, *101*, 1629 – 1658.
[11] P. R. Giunta, L. J. van de Burgt, A. E. Stiegman, *Chem. Mater.* **2005**, *17*, 1234 – 1240.

